Opto-Electronic Science

ISSN 2097-0382 CN 51-1800/O4

High performance micromachining of sapphire by laser induced plasma assisted ablation (LIPAA) using GHz burst mode femtosecond pulses

Kotaro Obata, Shota Kawabata, Yasutaka Hanada, Godai Miyaji and Koji Sugioka

Citation: Obata K, Kawabata S, Hanada Y, et al. High performance micromachining of sapphire by laser induced plasma assisted ablation (LIPAA) using GHz burst mode femtosecond pulses. *Opto-Electron Sci* **3**, 230053 (2024).

https://doi.org/10.29026/oes.2024.230053

Received: 31 December 2023; Accepted: 28 April 2024; Published online: 24 June 2024

Opto-Electronic Science

Article

June 2024, Vol. 3, No. 6

DOI: 10.29026/oes.2024.230053

High performance micromachining of sapphire by laser induced plasma assisted ablation (LIPAA) using GHz burst mode femtosecond pulses

Kotaro Obata[1], Shota Kawabata[1,2], Yasutaka Hanada[1,3], Godai Miyaji[2] and Koji Sugioka[1]*

GHz burst-mode femtosecond (fs) laser, which emits a series of pulse trains with extremely short intervals of several hundred picoseconds, provides distinct characteristics in materials processing as compared with the conventional irradiation scheme of fs laser (single-pulse mode). In this paper, we take advantage of the moderate pulse interval of 205 ps (4.88 GHz) in the burst pulse for high-quality and high-efficiency micromachining of single crystalline sapphire by laser induced plasma assisted ablation (LIPAA). Specifically, the preceding pulses in the burst generate plasma by ablation of copper placed behind the sapphire substrate, which interacts with the subsequent pulses to induce ablation at the rear surface of sapphire substrates. As a result, not only the ablation quality but also the ablation efficiency and the fabrication resolution are greatly improved compared to the other schemes including single-pulse mode fs laser direct ablation, single-pulse mode fs-LIPAA, and nanosecond-LIPAA.

Keywords: femtosecond laser; GHz burst mode; ablation; LIPAA; laser induced plasma assisted ablation; sapphire

Obata K, Kawabata S, Hanada Y et al. High performance micromachining of sapphire by laser induced plasma assisted ablation (LIPAA) using GHz burst mode femtosecond pulses. *Opto-Electron Sci* **3**, 230053 (2024).

Introduction

Over the past few decades, pulse shaping technology has become a potential tool to achieve better performance in laser materials processing[1–8]. In particular, GHz burst mode femtosecond (fs) laser, which emits a series of fs pulse trains with extremely short pulse intervals of several hundred picoseconds (ps), is recently attracting much attention for their ability to achieve high-performance materials processing in terms of quality, efficiency, and structure[9–23]. So far, we have demonstrated ablation of copper and silicon, which are typical materials of metals and semiconductors, respectively, to investigate ablation quality and efficiency by GHz burst mode fs laser[18–23]. When copper was ablated by the burst mode, we found that the plasma generated form copper by preceding laser pulses shields the subsequent pulses in the burst, resulting in reducing ablation efficiency compared to the conventional irradiation scheme (single-pulse mode)[18].

[1]RIKEN Center for Advanced Photonics (RAP), Wako-shi, Saitama 351-0198, Japan; [2]Faculty of Engineering, Tokyo University of Agriculture and Technology, Koganei, Tokyo 184-8588, Japan; [3]Graduate school of science and technology, Hirosaki University, Hirosaki, Aomori 036-8561, Japan.

*Correspondence: K Sugioka, E-mail: ksugioka@riken.jp

Received: 31 December 2023; Accepted: 28 April 2024; Published online: 24 June 2024

Although this result is unfavorable for high-efficiency ablation, it may be effective for a process based on interaction of laser and laser-induced plasma.

We have developed a technique termed laser induced plasma assisted ablation (LIPAA) in the 1990s for high-quality, high-efficiency microfabrication of transparent materials such as glass[24–28]. In the LIPAA process, a substrate that is transparent to the laser beam is placed on a metal target such as copper. The nanosecond (ns) pulsed laser is typically used, which is irradiated from the transparent substrate side. The laser beam first passes through the transparent material, and is then focused onto the metal target surface to generate plasma by ablation. Highly energetic species such as atoms and ions in the plasma collide with the rear surface of transparent substrate to induce electron excitation. The excited electrons cause transient absorption of the laser light by the rear surface of transparent substrate, resulting in ablation[26]. It should be noted that for ablation by LIPAA process, the plasma and laser beam have to be exposed at the rear surface of transparent substrate simultaneously. The plasma is typically generated tens to hundreds of ps after the laser irradiation on the metal and lasts several to tens of ns[27,28]. Therefore, ns lasers are a suitable light source for LIPAA, because almost the entire pulse can interact with the plasma. In contrast, when an fs laser is used for the LIPAA process, the fs laser cannot directly interact with the plasma, because the pulse irradiation is completed before the plasma is generated. In the case of fs laser, the process can proceed by two steps with multiple pulse irradiation. Specifically, a thin metal film is deposited on the rear surface of transparent material by 1st pulse of fs laser, and the 2nd and subsequent pulses are absorbed by the deposited metal thin film to induce ablation[27]. Consequently, the ablation efficiency using fs laser is much lower than ns-LIPAA.

In this paper, we propose to apply the GHz burst mode fs laser to LIPAA, because the moderate pulse interval in the GHz burst pulse could enable direct interaction of the subsequent laser pulses with plasma generated by the preceding laser pulses for high efficiency ablation. As with the normal ablation, GHz burst mode LIPAA is expected to be perform higher quality ablation compared to ns-LIPAA, in particular, wider bandgap materials such as sapphire. Single crystalline sapphire is an attractive material due to its excellent characteristics such as high-transparency in a visible range, high hardness (Mohs' scale of hardness 9), and good thermal resistivity beyond 2000 °C. In the industrial field, sapphire substrate is widely used as an ideal substrate for deposition of blue light-emitting diodes and other devices and for smart phone display panels. Sapphire is also used in medicine and blood chemistry[29]. However, sapphire is extremely hard and brittle, making high-quality, high-precision processing difficult. Furthermore, its high chemical stability prevents chemical etching except under extreme conditions. Standard processing of bulk sapphire substrate involves scribing with diamond-based tools and chemical-mechanical polishing. However, industry is demanding the development of higher precision, higher quality, and higher performance processing methods.

For high quality microprocessing of sapphire, dual-beam LIPAA was demonstrated, in which one fs laser beam was focused on the metal surface, while the other one was focused on the rear surface of sapphire[30]. An important feature of this process is the gap distance between the sapphire substrate and the metal target, which is longer than 150 μm. Therefore, in the dual-beam LIPAA, atoms and ions in the plasma induced by 1st pulse lose their energy during propagation, so that metal nanoparticles are deposited on the rear surface of sapphire substrate. Eventually, ablation takes place by absorption of 2nd pulse by the deposited nanoparticles. In contrast, GHz burst mode fs laser LIPAA will enable direct interaction of the plasma induced by the preceding laser pulses with the subsequent laser pulses, achieving higher ablation efficiency. Additionally, GHz burst mode fs laser LIPAA offers a simpler scheme compared to the dual-beam LIPAA. Thus, we show potential of GHz burst mode fs-LIPAA for high-quality, high-efficiency microfabrication of single crystalline sapphire substrates.

Methods

Figure 1(a) shows a schematic illustration of experimental setup for the GHz burst mode fs-LIPAA process. The LIPAA process using GHz burst mode was carried out using ultrashort laser pulses with a central wavelength of 1030 nm and a pulse duration of 215 fs. The Yb:KGW based high-power fs laser system (Pharos, Light Conversion Ltd.) enables to generate GHz burst pulses with the same wavelength and pulse width as the original fs laser pulse. The pulse energy was adjusted by using combination of the polarizing optics, which is composed of a lambda half waveplate and a polarizing beam splitter. For all experiments, a single burst pulse was incident on the

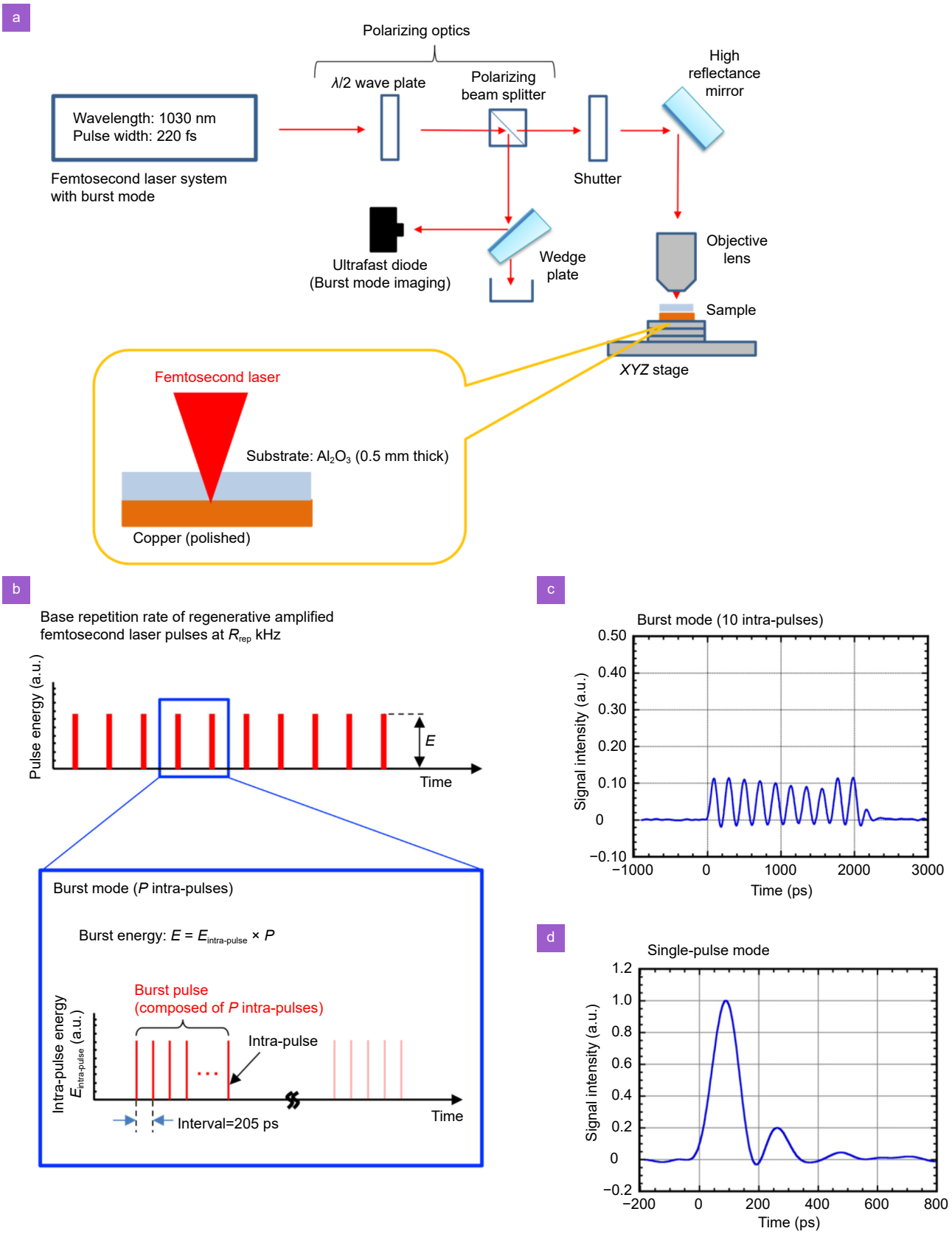

Fig. 1 | Schematic illustrations of (**a**) experimental setup for the GHz burst LIPAA process, (**b**) a pulse form of GHz burst mode containing *P* intra-pulses, and the measured waveforms of (**c**) a GHz burst pulse with 10 intra-pulse numbers and (**d**) a pulse at the single-pulse mode operation as comparison.

substrates, which was controlled by a mechanical shutter. As samples, c-axis (0001) oriented single crystalline sapphire substrates with a 0.5 mm thickness were used. The sapphire substrate was placed in contact with a copper target, and was then set on the computer controlled *XYZ* stage (OptSigma, OSMS20-85) to adjust the laser irradiation point. The linearly polarized laser beam that passed through the sapphire substrate was focused onto the copper target surface by a 20× objective lens with a numerical aperture (NA) of 0.45 (Olympus Ltd., LCPLN20XIR). The polarization direction of laser beam was parallel to crystallographic orientation (1120) of the single crystalline sapphire substrate. The focused spot-diameter on the copper surface was determined by using the formula for the relationship between the diameter of processed region and the fluence of Gaussian beam with experimental data[31,32] (Supplementary information, Fig. S1). The spot size of the laser was 3.77 μm when the laser beam was directly irradiated on copper. On the other hand, because the laser is irradiated through a sapphire substrate, which has a higher refractive index than air, the spot size of the LIPAA process is larger than direct irradiation, which was estimated at 5.35 μm.

In the burst mode, a packet of fs pulse train is called burst pulse, and each pulse in the burst pulse is called intra-pulse as shown in Fig. 1(b). We use the letter P to designate the number of intra-pulses in the burst pulse. The time separation between each intra-pulse was 205 ps, which corresponded to a repetition rate of 4.88 GHz. Both parameters of intra-pulse energy, $E_{\text{intra-pulse}}$ and burst pulse energy, E_{burst} were used for characterization, whose relationship is given by

$$E_{\text{burst}} = E_{\text{intra-pulse}} \times P\,. \tag{1}$$

As shown in Fig. 1(a), the polarizing beam splitter reflected part of the laser beam to direct it to an ultrafast photodiode (ET-3500, Electro-Optics Technology Inc.) connected to an oscilloscope (Infiniivision DSOX6002A, Keysight Technologies Inc.) for imaging the temporal beam profile of burst pulse. Figure 1(c) and 1(d) show the measured waveforms of GHz burst mode operation with P of 10 and the original single-pulse mode operation as comparison, respectively. In the GHz burst mode, energy of each intra-pulse was adjusted to be almost constant. The operation of GHz burst mode and the temporal distributions of laser pulse energy in the GHz burst mode have been described in detail elsewhere[18,20,22].

The morphology and the depth of ablated spots were evaluated by a scanning electron microscopy (SEM) and a laser scanning microscopy (LSM). However, when the ablation depth was much larger than the diameter of ablated crater, the depth could not be measured directly by the LSM because of the intense scattering of the LSM probe laser. Therefore, the replica method using a polydimethylsiloxane (PDMS) was employed to measure the ablated depths for those samples (Supplementary information, Fig. S2).

Results and discussion

Figure 2 shows the dependence of ablation depth on P in the GHz burst. The depth profiles of ablated craters were measured by LSM. As described above, when the created crater was too deep to obtain the cross-sectional profile by LSM directly, a negative structure was fabricated by the replica method using a polydimethylsiloxane (PDMS) and the height of replica was measured as the depth of crater for LIPAA process (Supplementary information, Fig. S2). The depths averaged from 10 samples for intra-pulse fluence $F_{\text{intra-pulse}}$ of 0.18, 0.22, 0.27, 0.36, 0.44 and 0.53 J/cm² are plotted in Fig. 2(a). All samples were fabricated by irradiation with a single burst pulse with P varied from 1 (single-pulse mode) to 10 as shown in Fig. 2(b). Naturally, variations of ablation depth on intra-pulse energy show that the higher $F_{\text{intra-pulse}}$ leads to

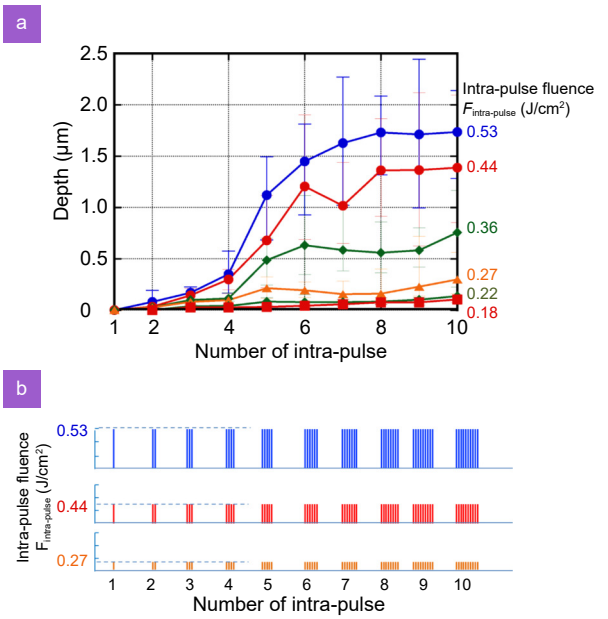

Fig. 2 | (**a**) Dependence of the ablated depth by GHz burst LIPAA process on the intra-pulse number in GHz burst pulse for the various intra-pulse fluence (0.18, 0.22, 0.27, 0.36, 0.44 and 0.53 J/cm²) and (**b**) pulse forms of GHz burst mode with various number of *P* intra-pulses.

increase of the ablation depth. For the same $F_{\text{intra-pulse}}$, the ablation depth increases with the number of intra-pulses, as a matter of course. However, the ablation depth drastically increases at P = 5, when the intra-pulse energy is larger than 0.27 J/cm^2. The reason for the drastic increase in ablation depth at P = 5 is thought to be that the plasma density becomes high enough to contribute LIPAA process at the timing of irradiation of the fifth intra-pulse. Specifically, the laser induced plasma is typically generated at the time scale of 10 ps ~ several ns after laser irradiation, which depends on materials and irradiation conditions. In case of Cu ablation, generation of the laser-induced plasma starts from 10–50 ps, and is then maximized at around 1 ns[33]. Additionally, our previous work demonstrating double-pulse fs-LIPAA has shown that the ablation depth drastically increases at the delay time of about 1 ns, and then decreases rapidly[27]. Considering the intra-pulse interval of 205 ps, it is reasonable that the ablation depth drastically increases for P = 5, since fifth intra-pulse is irradiated 820 ps after the first intra-pulse irradiation. Sixth and seventh intra-pulses can still interact with the dense plasma, which further increases the ablation depth (Seventh intra-pulse is irradiated 1.23 ns after the first intra-pulse irradiation). After about 1 ns, the density of plasma rapidly decreases, so that the interaction between plasma and the laser beam also decreases to suppress ablation. Furthermore, since most of the energy in fifth to seventh intra-pulses is consumed for ablation of the sapphire, the efficiency for generation of the laser induced plasma is significantly reduced. As a result, the eighth or later intra-pulses cannot interact with the dense plasma, resulting in little contribution for increasing the ablation depth. Consequently, the ablation depth is saturated at P = 8 or larger.

On the other hand, for $F_{\text{intra-pulse}}$ below 0.22 J/cm^2, significant ablation occurs for P = 3 or larger, but the ablation depth is much shallower compared to $F_{\text{intra-pulse}}$ above 0.27 J/cm^2, and the drastic increase at P = 5 is not observed. At these fluences, the energy of species in the plasma generated may be insufficient to directly interact with the laser beam Therefore, it's considered that the metal thin film deposited by preceding intra-pulses absorbs the energy of the subsequent intra-pulses to induce ablation, resulting in much smaller ablation efficiency. In order to deposit the metal film thick enough to induce ablation, two intra-pulses or a time interval longer than 410 ps may be necessary.

Dependence of ablated depth on $F_{\text{intra-pulse}}$ for GHz burst mode LIPAA is investigated to be compared to the single-pulse mode direct ablation (Fig. 3(a)) and single-pulse mode LIPAA (Fig. 3(b)). The schematic schemes with pulse forms of each process are also shown in Fig. 3(c). In this experiment, a single burst pulse containing 10 intra-pulses was used for the GHz burst mode, while 10 pulses of fs laser with the same fluence as the $F_{\text{intra-pulse}}$ in GHz burst were irradiated at a repetition rate of 10 Hz for both single-pulse mode processing. In Fig. 3(a), the GHz burst LIPAA process can be classified into two regimes in terms of the slope of the energy dependence of ablation depth with $F_{\text{intra-pulse}}$ bordered by 0.22 J/cm^2. Specifically, the regime 1 with a smaller slope below 0.22 J/cm^2 is attributed to direct etching by laser-induced plasma which contains highly energetic species generated by higher peak intensity of fs laser, while the regime 2 with a much larger slope above 0.22 J/cm^2 is due to contribution of LIPAA. Thus, the threshold pulse energy for LIPAA by GHz burst mode is estimated to be 0.22 J/cm^2. Meanwhile, the threshold pulse energy for the single-pulse mode direct ablation is 1.61 J/cm^2, indicating that the GHz burst LIPAA process enables to reduce the threshold fluence to 1/7.3 of the single-pulse mode direct ablation. The great reduction of threshold fluence can be deduced that the plasma generated by the ablation of the copper target with preceding intra-pulses transiently induce strong absorption of the subsequent intra-pulses by the rear surface of sapphire substrate, as described above. In the light-matter interaction conditions involving nonlinear effects by the ultrafast laser pulse, peak intensity and wavelength are especially important parameters. In this experiment, the wavelength of 1030 nm was used as the light source, which is transparent to single crystalline sapphire substrate. Therefore, ablation of sapphire by 1030 nm wavelength fs laser is only possible by 8 photon absorption due to 8.64 eV of bandgap of sapphire[34]. Such high order multiphoton absorption should require much higher laser fluence for processing[35] and then deteriorate the ablation quality as shown later. In the meanwhile, almost linear increase of the ablation depth for the logarithm of laser fluence at the regime 2 of the GHz burst LIPAA suggests ablation by single photon absorption, which should be responsible for high-efficiency, high-quality ablation.

As seen in Fig. 3(b), the GHz burst mode LIPAA and the single-pulse mode LIPPA show almost similar ablation depth up to 0.22 J/cm^2 of $F_{\text{intra-pulse}}$. This can be

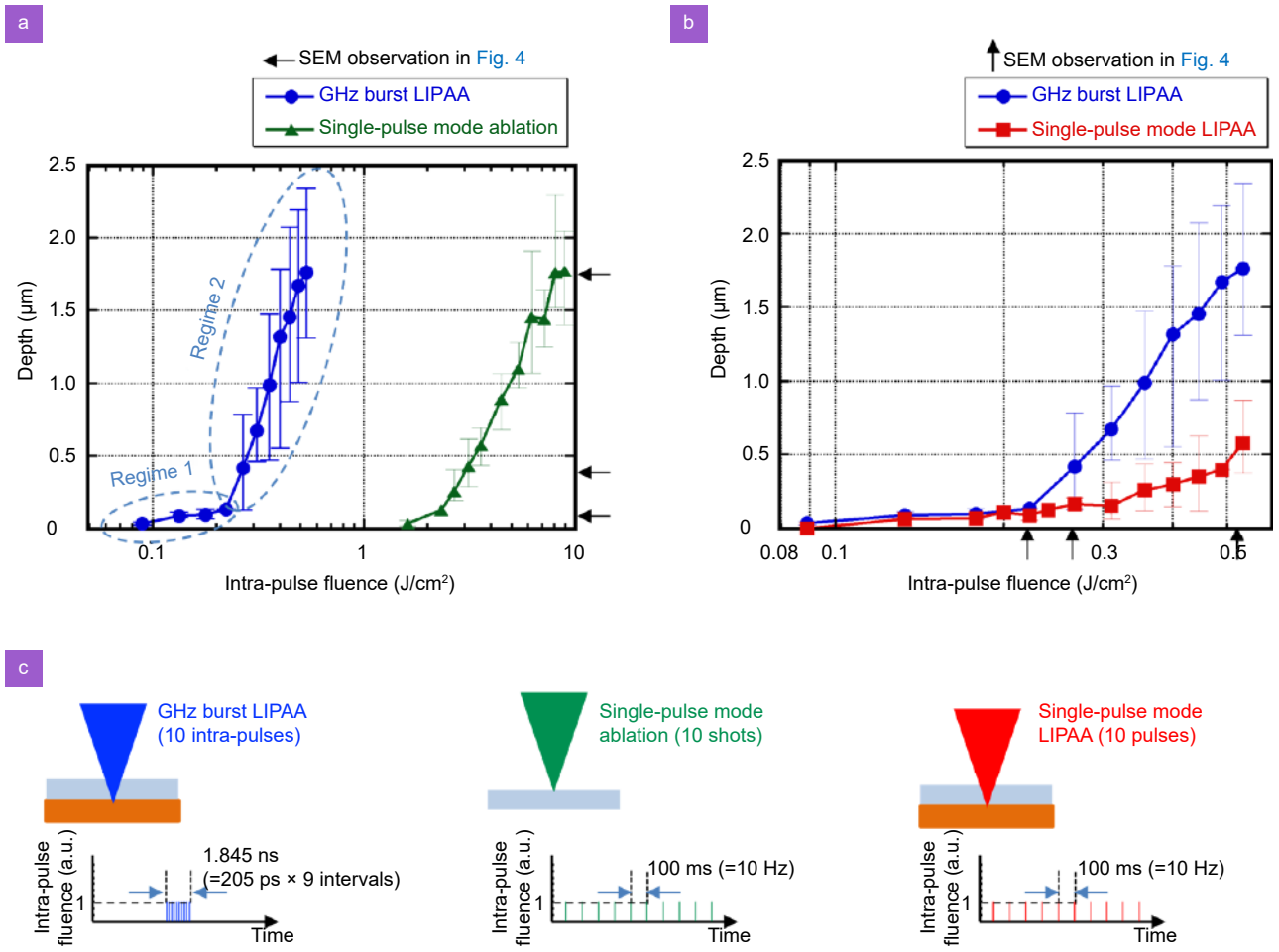

Fig. 3 | Dependence of ablation depth on laser fluence for (**a**) GHz burst LIPAA process (circle, *P*=10, 1 shot) and conventional single-pulse mode direct ablation (triangle, 10 shots) and (**b**) GHz burst LIPAA process (circle, *P*=10, 1 shot) and single-pulse mode LIPAA process (square, 10 shots). Schematic schemes with pulse forms of each process are illustrated below graphs.

Table 1 | Ablation efficiency of GHz burst LIPAA (*P*=10, 1 shot), single-pulse mode ablation (10 shots), and single-pulse mode LIPAA (*P*=10, 1 shot) for the ablation depth of 0.5 μm.

	GHz burst LIPAA (10 intra-pulses)	Single-pulse mode ablation (10 shots)	Single-pulse mode LIPAA (10 pulses)
Intra-pulse fluence at 0.5 μm of depth [J/cm ²]	0.440	2.65	0.905
Ablation efficiency [μm/J/cm ²]	1.14	0.19	0.55

explained by the fact that direct etching with laser-induced plasma is the dominant process in this regime. Above 0.22 J/cm², the slop becomes somewhat larger for the single-pulse mode LIPPA, but is much smaller than that for the GHz burst mode LIPAA. Quantitatively, the ablation depth by the GHz burst mode LIPAA is 4.2–5.0 times deeper than that by the single-pulse mode LIPAA at $F_{\text{intra-pulse}}$ of 0.27–0.53 J/cm². As described above, the single-pulse mode LIPAA takes place by a two-step process. Specifically, a metal thin film is first deposited on the sapphire substrate by ablation of copper target by preceding intra-pulses, and the subsequent intra-pulses are absorbed by the deposited copper thin film to induce ablation. Meanwhile, in the GHz burst mode LIPAA, direct interaction of laser beam with the laser-induced plasma can significantly increase the absorption on sapphire surface to create deeper craters, resulting in high-efficiency ablation.

For more quantitative evaluation of the ablation efficiency, we defined it as the ablation depth per unit fluence. To compare the ablation efficiency between GHz burst LIPAA process and the other methods, they were calculated using the laser fluence at the ablation depth of 0.5 μm for each method shown in Fig. 3, and were summarized in Table 1. The ablation efficiency by the GHz burst mode LIPAA is 1.14 μm/J/cm² which is 6.0 and 2.1

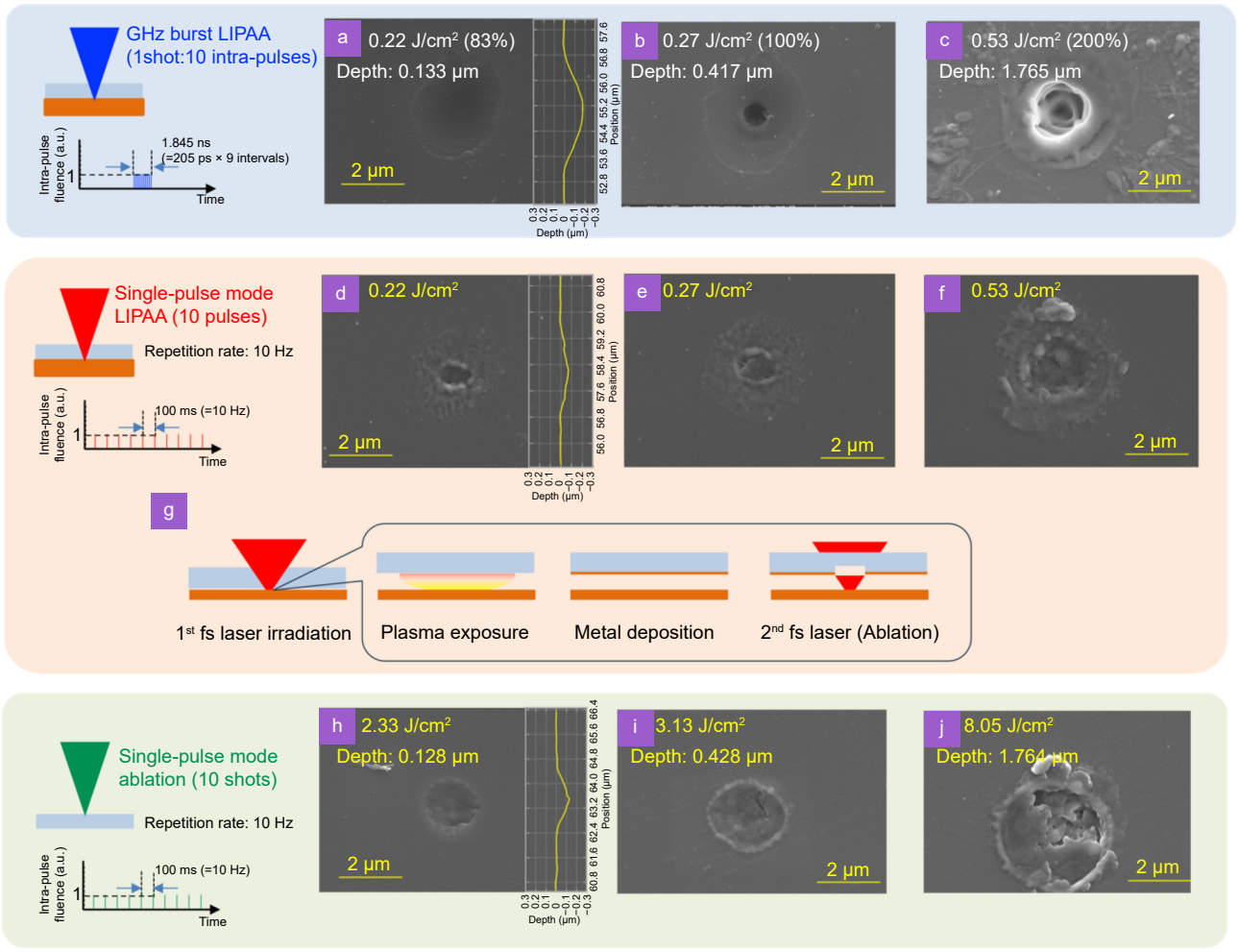

Fig. 4 | SEM images of ablated spots on the sapphire surfaces with different configurations: GHz burst LIPAA (P= 10) at intra-pulse fluence of (**a**) 0.22 J/cm², (**b**) 0.27 J/cm², and (**c**) 0.53 J/cm², single-pulse mode LIPAA (10 shots of fs laser pulses at a repetition rate of 10 Hz) at same intra-pulse fluence of (**d**) 0.22 J/cm², (**e**) 0.27 J/cm², and (**f**) 0.53 J/cm² with (**g**) schematic scheme of two-step process, and single-pulse mode direct fs laser ablation at laser fluences of (**h**) 2.33 J/cm², (**i**) 3.13 J/cm², and (**j**) 8.05 J/cm². Schematic illustrations of each scheme are shown at left side of SEM images.

times higher than that by the single-pulse mode direct ablation and the single-pulse mode LIPAA, respectively.

The morphologies of ablated craters created on sapphire substrate by different schemes of laser irradiation were observed by SEM. Figure 4(a–c) show SEM images of the ablated spots created by GHz burst mode LIPAA process (single shot of GHz burst pulse with P= 10)) at $F_{\text{intra-pulse}}$ of 0.22, 0.27 and 0.53 J/cm², respectively. As a comparison, the results obtained by LIPAA with single-pulse mode and single-pulse mode fs laser direct ablation are also shown in Fig. 4(d–f) and Fig. 4(h–j) , respectively (10 shots of fs laser pulses at a repetition rate of 10 Hz). The schematics of irradiation schemes (upper) and pulse forms (lower) are also shown at the left side of SEM images.

For GHz burst mode LIPAA process, the sapphire substrate surface irradiated at $F_{\text{intra-pulse}}$ of 0.22 J/cm² shows shallow crater with a diameter of 3.2 μm (Fig. 4(a)). The cross-sectional profile of created crater measured by LSM is displayed at the right side of SEM image. The crater diameter is smaller than the laser spot size (5.35 μm). As $F_{\text{intra-pulse}}$ increases to 0.27 J/cm², a deep crater, whose diameter of 0.78 μm is much smaller than the laser spot size, is obviously created at the center in the shallow etch region (Fig. 4(b)). The created crater was too deep to measure the cross-sectional profile by LSM, so that no cross-sectional profile of hole prepared at 0.27 J/cm² is displayed. The diameter of shallow etch region increases slightly as compared with Fig. 4(a). As $F_{\text{intra-pulse}}$ increases by a factor of 2 from 0.27 J/cm² to 0.53 J/cm², the deep crater diameter is widened by a factor of 2.2 from 0.78 μm to 1.73 μm (Fig. 4(c)). Importantly, the diameter of ablation hole at 0.53 J/cm² is still much smaller than 5.35 μm of the laser spot size due to

the synergetic contribution of threshold effect and higher plasma density closer to the center of laser beam as discussed below. If the deeper hole with the smaller diameter is required, multiple pulse irradiation with lower power should be implemented, although it will affect the processing speed. The increase in both the crater diameter and the depth with increasing the laser power is a common characteristic in laser ablation. In fact, the conventional direct fs laser ablation shows the same phenomena (see Fig. 4(h–j)). Importantly, the GHz burst mode LIPAA can create the deeper hole with the smaller diameter faster than the fs laser direct ablation due to its higher ablation efficiency. As described in Fig. 3(a), the shallow etching may be caused by direct etching by the laser-induced plasma. The etching region smaller than the laser spot size can be explained by the fact that the plasma closer to the center of the laser beam, where the plasma density is higher, can contribute more to ablation. Thus, the larger pulse energy creates larger etching region due to larger area of high plasma density. However, such shallow etching is undesirable in many applications. The shallow etching may be avoided by introducing a gap with a distance of hundred μm between the substrate and the metal target, because the energy of species is decreased during the propagation. Even with such a gap, LIPAA can work[28]. Meanwhile, $F_{\text{intra-pulse}}$ of 0.22 J/cm^2 may be below the ablation threshold by LIPAA, so that the deep hole is not created. Increasing $F_{\text{intra-pulse}}$ to 0.27 J/cm^2 can exceed the threshold for LIPAA, resulting in creation of deep hole at the center of laser irradiated region. The ablated diameter far beyond the focused laser spot size (< one-sixth) is due to the threshold effect when using the Gaussian beam[36]. Specifically, ablation can take place only at the center of Gaussian beam where the laser intensity exceeds the ablation threshold. The threshold effect to achieve the higher resolution is more effective for LIPAA compared to the direct ablation, because the density of laser-induced plasma which affects the ablation threshold should be higher closer to the center of laser beam. The synergetic effect can highly contribute to achieve the fabrication resolution far beyond the focused laser spot size by GHz burst mode LIPAA.

Meanwhile, the single-pulse mode LIPAA creates larger craters at the same $F_{\text{intra-pulse}}$ as shown in Fig. 4(d–f) . Furthermore, the ablated surfaces are significantly roughened compared to the GHz burst mode. The better ablation quality by the GHz burst mode than the single-pulse mode is because the plasma induced by the preceding intra-pulses in the burst can induce efficient absorption at the rear surface of sapphire by the subsequent intra-pulses due to proper pulse interval in GHz range. It's known that higher absorption is essential for better ablation quality. In contrast, for the single-pulse mode LIPAA, the plasma induced by the preceding pulse is extinguished before the subsequent laser pulse arrives at the sapphire substrate, which makes the direct interaction of laser and plasma impossible as already discussed above. Therefore, the two-step process shown in Fig. 4(g) is only possible; 1) a thin metal film is deposited on the rear surface of sapphire substrate from the plasma induced by the preceding laser pulse; 2) the subsequent laser pulse is absorbed by the deposited film to cause ablation[26]. Compared to the GHz burst mode, the wider width and the shallower depth of crater as well as worse ablation quality may be due to ablation by diffusion of heat generated by absorption of laser energy by the deposited metal thin film. Hence, we conclude that GHz burst mode is much more effective for LIPAA process by fs laser to achieve higher efficiency, higher quality, and better resolution in fabrication.

For the single-pulse mode fs laser direct ablation (Fig. 4(h–j)), the laser fluences were set such that the crater depths are almost the same as those for the GHz burst mode LIPAA samples. For the crater depth of ~0.13 μm (Fig. 4(a, h)), the diameter created by single-pulse mode fs laser direct ablation is smaller than the GHz burst mode LIPAA probably due to synergetic contribution of the threshold effect and the effective spot size caused by 8 photon absorption[36]. In contrast, for the crater depth of ~0.43 μm (Fig. 4(b, i)), the diameter by single-pulse mode fs laser direct ablation is obviously larger than that of deep crater fabricated by the GHz burst LIPAA process, which would indicate that the synergetic contribution of threshold effect and plasma density distribution for the GHz burst LIPAA process is much more effective than decreased effective spot size due to multiphoton absorption to achieve higher fabrication resolution. As the laser fluence increases by a factor of 2 (Fig. 4(c, j)), the crater diameter further increases to 3.68 μm. The bottom surfaces of the craters created by the single-pulse mode fs laser direct ablation are much more roughened compared to those by the GHz burst LIPAA process. Additionally, significant swelling at the ablated edges due to melting are observed, while no swelling occurs for the GHz burst mode LIPAA samples. Thus, we can conclude that GHz burst mode LIPAA process can achieve much better ablation quality with improved fabrication

resolution as compared with the direct fs laser ablation. We further performed ns-LIPAA, showing significant melting due to thermal effect (Supplementary information, Fig. S3). Regarding the effect of polarization direction, it affects some types of processing such as laser-induced periodic surface strictures or LIPSS formation[22,23] and nanoscale precise-3D structuring by two-photon polymerization[37]. However, to the best of our knowledge, it has little effect on relatively large-scale ablations. In fact, we didn't observe any effect of polarization direction in all ablation schemes.

We have also applied GHz bust mode to LIPAA of glass slide, and obtained the similar results as sapphire in comparison with the other irradiation schemes. We believe that the GHz burst mode LIPAA could be effective for other transparent materials. Meanwhile, other materials such as stainless steel, silver, and silicon can be used as targets for LIPAA process, as long as they are strongly absorbed by the laser beam used[24,38]. However, the characteristics of generated plasma depend on the type of target materials, which should affect the characteristics of ablation.

In principle, direct writing with the focused laser beam scanned in a plane perpendicular to the substrate can be applied to LIPAA for flexible surface pattering[39], which will be also effective for GHz burst mode LIPAA. In the GHz burst LIPAA process, the subsequent pulses in the burst pulse must be precisely injected onto the area of sapphire where the high-density plasma induced by the preceding intra-pulses is exposed. Even if the focused laser beam is scanned, the subsequent intra-pulses can be focused on such a high-density plasma region because of the very short duration of the intra-pulses. For example, when the scanning speed is 1000 mm/sec, the movement distance of focused laser beam during the burst pulse irradiation from the first intra-pulse to the tenth intra-pulse is only 1000 mm/s × (205 × 10^{-12} s × 9) = 1.85 nm. This is only 0.035 % of the beam spot (5.35 μm) and can be therefore negligible. On the other hand, scanning the focused laser beam along the beam axis to create deep hole affects the ablation performance, because the plasma density decreases as the ablation spot is away from the target surface. This is the common characteristics of LIPAA.

Conclusion

Fs laser GHz burst mode has revolutionized laser materials processing with its improved processing quality and enhanced ablation efficiency. In this paper, we have applied GHz burst mode processing to LIPAA process of sapphire substrates. Moderate pulse interval of several hundred ps in the burst enabled direct interaction between the fs laser pulses and the laser-induced plasma, resulting in strong absorption of the laser beam by the sapphire substrates. Consequently, the ablation threshold was decreased to 1/7.3 compared with the single-pulse mode fs laser direct ablation. In addition, the ablation depth was increased by a factor of 4.2–5.0 times compared to that by the single-pulse mode LIPAA. The increased absorption further allowed us to achieve much better ablation quality than other schemes including ns-LIPAA. Additionally, GHz burst mode achieves the fabrication resolution far beyond the focused laser spot size due to the synergetic contribution of threshold effect and higher plasma density closer to the center of laser beam. Thus, it can be concluded that the GHz burst mode LIPAA process provide the ability to realize micro- and nanofabrication of sapphire with high processing efficiency, high processing quality, and high fabrication resolution. This process can be further extended to processing of other transparent materials. Furthermore, the use of shaped beams such as Bessel beam and vector beam could enhance the performance of LIPAA in terms of fabrication geometry, resolution and efficiency.

References

1. Zhang YC, Jiang QL, Long MQ et al. Femtosecond laser-induced periodic structures: mechanisms, techniques, and applications. *Opto-Electron Sci* **1**, 220005(2022).
2. Chen LW, Hong MH. Laser surface structuring of semiconductors and functionalization. In Sugioka K. *Handbook of Laser Micro- and Nano-Engineering* (Cham: Springer, 2021).
3. Zhang DS, Li XZ, Fu Y et al. Liquid vortexes and flows induced by femtosecond laser ablation in liquid governing formation of circular and crisscross LIPSS. *Opto-Electron Adv* **5**, 210066(2022).
4. Fraggelakis F, Tsibidis GD, Stratakis E. Ultrashort pulsed laser induced complex surface structures generated by tailoring the melt hydrodynamics. *Opto-Electron Adv* **5**, 210052(2022).
5. Zhang YC, Jiang QL, Cao KQ et al. Extremely regular periodic surface structures in a large area efficiently induced on silicon by temporally shaped femtosecond laser. *Photon Res* **9**, 839–847(2021).
6. Jiang QL, Zhang YC, Xu YF et al. Extremely high-quality periodic structures on ITO film efficiently fabricated by femtosecond pulse train output from a frequency-doubled Fabry-Perot cavity. *Nanomaterials* **13**, 1510(2023).
7. He F, Yu JJ, Tan YX et al. Tailoring femtosecond 1.5-μm Bessel beams for manufacturing high-aspect-ratio through-silicon vias. *Sci Rep* **7**, 40785(2017).
8. Zhang JW, Obata K, Ozasa K et al. Rapid manufacturing of glass-based digital nucleic acid amplification chips by ultrafast Bessel pulses. *Small Sci* **4**, 2300166(2024).
9. Kerse C, Kalaycıoğlu H, Elahi P et al. Ablation-cooled material removal with ultrafast bursts of pulses. *Nature* **537**, 84–88(2016).

10. Mishchik K, Bonamis G, Qiao J et al. High-efficiency femtosecond ablation of silicon with GHz repetition rate laser source. *Opt Lett* **44**, 2193–2196(2019).
11. Bonamis G, Audouard E, Hönninger C et al. Systematic study of laser ablation with GHz bursts of femtosecond pulses. *Opt Express* **28**, 27702–27714(2020).
12. Metzner D, Lickschat P, Weißmantel S. High-quality surface treatment using GHz burst mode with tunable ultrashort pulses. *Appl Surf Sci* **531**, 147270(2020).
13. Hodgson N, Allegre H, Starodoumov A et al. Femtosecond laser ablation in burst mode as a function of pulse fluence and intra-burst repetition rate. *J Laser Micro Nanoeng* **15**, 236–244(2020).
14. Metzner D, Lickschat P, Weißmantel S. Optimization of the ablation process using ultrashort pulsed laser radiation in different burst modes. *J Laser Appl* **33**, 012057(2021).
15. Žemaitis A, Gaidys M, Gečys P et al. Femtosecond laser ablation by bibursts in the MHz and GHz pulse repetition rates. *Opt Express* **29**, 7641–7653(2021).
16. Matsumoto H, Lin ZB, Schrauben JN et al. Ultrafast laser ablation of silicon with ~GHz bursts. *J Laser Appl* **33**, 032010(2021).
17. Förster DJ, Jäggi B, Michalowski A et al. Review on experimental and theoretical investigations of ultra-short pulsed laser ablation of metals with burst pulses. *Materials* **14**, 3331(2021).
18. Obata K, Caballero-Lucas F, Sugioka K. Material processing at GHz burst mode by femtosecond laser ablation. *J Laser Micro Nanoeng* **16**, 19–23(2021).
19. Sugioka K. Will GHz burst mode create a new path to femtosecond laser processing. *Int J Extrem Manuf* **3**, 043001(2021).
20. Caballero-Lucas F, Obata K, Sugioka K. Enhanced ablation efficiency for silicon by femtosecond laser microprocessing with GHz bursts in MHz bursts (BiBurst). *Int J Extrem Manuf* **4**, 015103(2022).
21. Obata K, Caballero-Lucas F, Kawabata S et al. GHz bursts in MHz burst (BiBurst) enabling high-speed femtosecond laser ablation of Silicon due to prevention of air ionization. *Int J Extrem Manuf* **5**, 025002(2023).
22. Kawabata S, Bai S, Obata K et al. Two-dimensional laser-induced periodic surface structures formed on crystalline silicon by GHz burst mode femtosecond laser pulses. *Int J Extrem Manuf* **5**, 015004(2023).
23. Kawabata S, Bai S, Obata K et al. Formation of two-dimensional laser-induced periodic surface structures on titanium by GHz burst mode femtosecond laser pulses. *Front Nanotechnol* **5**, 1267284(2023).
24. Zhang J, Sugioka K, Midorikawa K. Direct fabrication of micro-gratings in fused quartz by laser-induced plasma-assisted ablation with a KrF excimer laser. *Opt Lett* **23**, 1486–1488(1998).
25. Zhang J, Sugioka K, Midorikawa K. High-quality and high-efficiency machining of glass materials by laser-induced plasma-assisted ablation using conventional nanosecond UV, visible, and infrared lasers. *Appl Phys A* **69**, S879–S882(1999).
26. Hanada Y, Sugioka K, Obata K et al. Transient electron excitation in laser-induced plasma-assisted ablation of transparent materials. *J Appl Phys* **99**, 043301(2006).
27. Hanada Y, Sugioka K, Miyamoto I et al. Double-pulse irradiation by laser-induced plasma-assisted ablation (LIPAA) and mechanisms study. *Appl Surf Sci* **248**, 276–280(2005).
28. Hanada Y, Sugioka K, Gomi Y et al. Development of practical system for laser-induced plasma-assisted ablation (LIPAA) for micromachining of glass materials. *Appl Phys A* **79**, 1001–1003(2004).
29. Buschow KH, Cahn RW, Flemings MC et al. Properties, growth and applications. *Encyclopedia of Materials: Science and Technology* (Amsterdam: Elsevier, 2001).
30. Li Y, Liu HG, Hong MH. High-quality sapphire microprocessing by dual-beam laser induced plasma assisted ablation. *Opt Express* **28**, 6242–6250(2020).
31. Liu JM. Simple technique for measurements of pulsed Gaussian-beam spot sizes. *Opt Lett* **7**, 196–198(1982).
32. Žemaitis A, Gaidys M, Brikas M et al. Advanced laser scanning for highly-efficient ablation and ultrafast surface structuring: experiment and model. *Sci Rep* **8**, 17376(2018).
33. Förster DJ, Faas S, Gröninger S et al. Shielding effects and redeposition of material during processing of metals with bursts of ultra-short laser pulses. *Appl Surf Sci* **440**, 926–931(2018).
34. Heath DF, Sacher PA. Effects of a simulated high-energy space environment on the ultraviolet transmittance of optical materials between 1050 Å and 3000 Å. *Appl Opt* **5**, 937–943(1966).
35. Skliutas E, Samsonas D, Čiburys A et al. X-photon laser direct write 3D nanolithography. *Virtual Phys Prototyp* **18**, e2228324(2023).
36. Sugioka K, Cheng Y. Ultrafast lasers—reliable tools for advanced materials processing. *Light Sci Appl* **3**, e149(2014).
37. Rekštytė S, Jonavičius T, Gailevičius D et al. Nanoscale precision of 3D polymerization via polarization control. *Adv Opt Mater* **4**, 1209–1214(2016).
38. Hong MH, Sugioka K, Lu YF et al. Laser microfabrication of transparent hard materials and signal diagnostics. *Appl Surf Sci* **186**, 556–561(2002).
39. Hong MH, Sugioka K, Wu DJ et al. Laser-induced-plasma-assisted ablation for glass microfabrication. *Proc SPIE* **4595**, 138–146(2001).

Acknowledgements

The authors would like to thank the Materials Characterization Support Team, RIKEN CEMS for providing access to the SEM. This work was supported by MEXT Quantum Leap Flagship Program (MEXT Q-LEAP) Grant Number JPMXS0118067246.

Author contributions

K Obata and K Sugioka designed the research; K Obata, S Kawabata, and Y Hanada conducted experimental research; G Miyaji and K Sugioka supervised the research; and K Obata and K Sugioka wrote the paper.

Competing interests

The authors declare no competing financial interests.

Supplementary information

Supplementary information for this paper is available at https://doi.org/10.29026/oes.2024. 230053

Scan for Article PDF